

The Relationship among Hypoxia, Proliferation, and Outcome in Patients with De Novo Glioblastoma: A Pilot Study¹

Sydney M. Evans*, Kevin W. Jenkins*, H. Isaac Chen[†], W. Timothy Jenkins*, Kevin D. Judy[†], Wei-Ting Hwang[‡], Robert A. Lustig*, Alexander R. Judkins[§], M. Sean Grady[†], Stephen M. Hahn* and Cameron J. Koch*

*Department of Radiation Oncology, University of Pennsylvania School of Medicine, Philadelphia, PA, USA; [†]Department of Neurosurgery, University of Pennsylvania School of Medicine, Philadelphia, PA, USA; [‡]Department of Epidemiology and Biostatistics, University of Pennsylvania School of Medicine, Philadelphia, PA, USA; [§]Department of Pathology, Children's Hospital of Philadelphia, Philadelphia, PA, USA

Abstract

The hypoxia and proliferation index increase with grade in human glial tumors, but there is no agreement whether either has prognostic importance in glioblastomas. We evaluated these end points individually and together in 16 *de novo* human glioblastomas using antibodies against the 2-nitroimidazole hypoxia detection agent EF5 and the proliferation detection agent Ki-67. Frozen tumor tissue sections were fluorescence-stained for nuclei (Hoechst 33342), hypoxia (anti-EF5 antibodies), and proliferation (anti-Ki-67 antibodies). EF5 binding adjacent to Ki-67+ cells, overall EF5 binding, the ratio of these values, and the proliferation index were evaluated. Patients were classified using recursive partitioning analysis and followed up until recurrence and/or death. Recursive partitioning analysis was statistically significant for survival ($P = .0026$). Overall EF5 binding, EF5 binding near Ki-67+ cells, and proliferation index did not predict recurrence. Two additional survival analyses based on ratios of the overall EF5 binding to EF5 binding near Ki-67+ cells were performed. High and low ratio values were determined by two cutoff points: (a) the 50% value for the ratio $[EF5/Ki-67_{\text{Binding}}]/[Tumor_{\text{binding}}] = \text{Ratio}_{EF5\ 50\%}$ and (b) the median EF5 value (75.6%) of the ratio $[EF5/Ki-67_{\text{Binding}}]/[Tumor_{\text{binding}}] = \text{Ratio}_{\text{patients median}}$. On the basis of the $\text{Ratio}_{EF5\ 50\%}$, recurrence ($P = .0074$) and survival ($P = .0196$) could be predicted. Using the $\text{Ratio}_{\text{patients median}}$, only survival could be predicted ($P = .0291$). In summary, patients had a worse prognosis if the $[EF5/Ki-67_{\text{Binding}}]/[Tumor_{\text{binding}}]$ ratio was high. A hypothesis for the mechanisms and translational significance of these findings is discussed.

Translational Oncology (2010) 3, 160–169

Introduction

Glioblastoma (GB) is one of the deadliest of human cancers, characterized by a 12- to 14-month median survival in patients treated with surgery, radiation, and temozolomide [1]. There is extensive ongoing research on the mechanism(s) of this dismal prognosis, including the role of signaling molecules, cytokines, and drug-modifying enzymes [2]. Several of these factors are modulated by hypoxia, leading to substantial clinical and experimental interest in this subject [3]. Hypoxia is present in many tumor sites including cervix, head and neck, prostate, bladder, pancreas, and soft tissue sarcomas (for review, see Evans and Koch [4]). Hypoxia has also been shown to affect the efficacy of

chemotherapy [5]. In some tumor types (cervical cancer, sarcomas), it is associated with tumor aggression, for example, hypoxic tumors

Address all correspondence to: Sydney M. Evans, VMD, University of Pennsylvania, Department of Radiation Oncology, 195 John Morgan Bldg, 37th St and Hamilton Walk, Philadelphia, PA 19104-6072. E-mail: sydevans@mail.med.upenn.edu

¹This study was supported by National Institutes of Health grants RO1 CA 75285, RO1 CA 113561, and R21 CA 93007 (to S.M. Evans, PI).

Received 4 September 2009; Revised 14 December 2009; Accepted 15 December 2009

Copyright © 2010 Neoplasia Press, Inc. All rights reserved 1944-7124/10/\$25.00
DOI 10.1593/tlo.09265

are more likely to invade and/or metastasize [6,7] as a result of up-regulation of proteins such as matrix metalloproteinase, vascular endothelial growth factor, and BCL-XL [6–8]. We have previously reported on the presence and level of hypoxia in a series of brain tumors of varying histologic diagnosis, demonstrating that the level of hypoxia increases with tumor aggressiveness [9]. However, tissue PO_2 has never been demonstrated to be a predictive factor in the outcome of patients with GB. Proliferation, another well-studied physiologic process in tumors, remains controversial as to its prognostic significance in GBs [10–12].

EF5 is a 2-nitroimidazole drug that is administered intravenously to patients approximately 24 hours preceding surgery. It covalently binds to hypoxic cells at a rate that is inversely proportional to tissue PO_2 [13,14]. Analytical methods using highly specific, fluorescent monoclonal antibodies against EF5 adducts have been developed, calibrated to *in vitro* controls, and validated, allowing the quantification of tissue oxygen levels and the production of tissue oxygen maps [15]. Immunohistochemical (IHC) studies have generally reported an inverse spatial relationship between hypoxic and proliferating cells [16,17], but we noticed that proliferating (Ki-67–positive [Ki-67+]) cells could be found in regions of high EF5 binding in many human GB tissue sections (Figure 1). This has been previously observed in liver metastases [18]. On the basis of our observation of colocalization of hypoxic and proliferating cells, we developed quantitative methods using frozen tissue sections to analyze the cellular PO_2 from tissue sections in the region immediately surrounding any defined anatomic structure (e.g., blood vessels [19] or individual cells [present studies]). Herein, we describe the development and application of such algorithms to quantitatively assess EF5 binding in the region of Ki-67+ cells. We hypothesized that tumors with many proliferating hypoxic cells would be more biologically aggressive, perhaps due to the up-regulation of invasion and metastasis-causing cytokines. In this pilot study, we provide data supporting that the EF5 binding level surrounding proliferating cells, expressed as a ratio

$[EF5/Ki-67_{binding}]/[Tumor_{binding}]$, is a significant predictor of patient outcome. We also showed that this ratio variable can independently predict these end points beyond the recursive partitioning analysis (RPA) classification [20]. (The RPA classification is based on both pretreatment patient and tumor characteristics and treatment-related variables, and it has been shown to be associated with survival duration.) Measurement of the relationship between hypoxia and proliferation in GBs is not likely to be directly applicable to clinical practice using the complex methods described herein. However, these techniques should inform the biology and pathophysiology of GBs for future investigations as well as aid the development of molecular and imaging therapeutics.

Materials and Methods

The Institutional Review Board of the University of Pennsylvania Clinical Trials and Scientific Monitoring Committee (Abramson Cancer Center) and the Cancer Therapeutics Evaluation Program of the National Cancer Institute approved this prospective trial of EF5. All patients signed a consent form for both the study and for privacy (Health Insurance Portability Accountability Act). Patients of all ethnic and sex groups were included. Eligible patients were those undergoing resection of a brain mass assessed as likely to be a neoplasm based on imaging appearance. Exclusion criteria included patients with a history of grade 3 or 4 peripheral neuropathy [21], pregnant or nursing patients, and patients younger than 18 years.

EF5 Administration

The National Cancer Institute, Division of Cancer Treatment, supplied EF5 in 100-ml vials containing an aqueous solution of 3 mg/ml EF5 plus 5% dextrose and 2.4% ethanol. EF5 was administered through a peripheral intravenous catheter approximately 24 hours before surgery at a rate no greater than 350 ml/h and to a total dose of

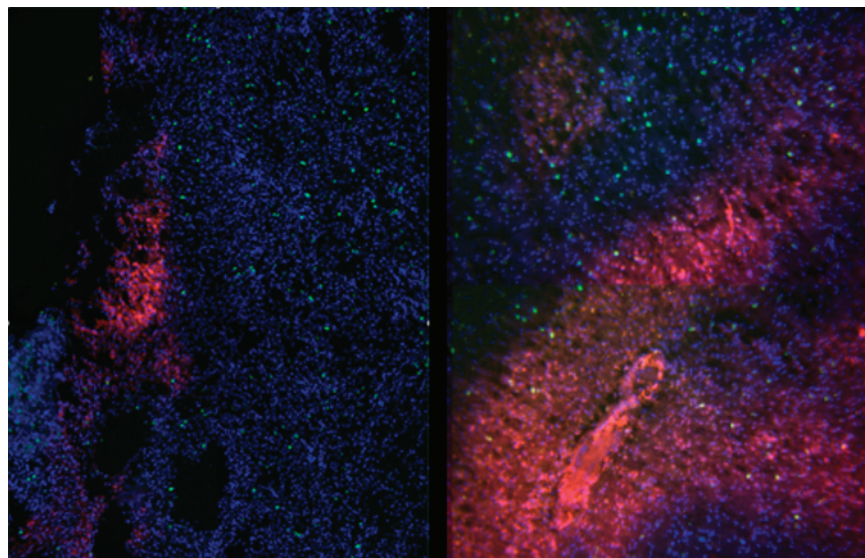


Figure 1. Examples of EF5, Ki-67 (proliferation), and Hoechst 33342 (viable cells) binding in GBs. Color codes: hypoxia (EF5 binding, red), viable cells (Hoechst 33342, blue) and proliferation (Ki-67, green). Left panel: patient 39; right panel: patient 55. Both patients have regions of moderate hypoxia, but in patient 39, all proliferating cells are in oxic regions compared with patient 55, where proliferating hypoxic cells are seen. It should be noted that yellow cells in this image are moderately hypoxic and proliferating, but many proliferating cells close to the moderately hypoxic regions are mildly hypoxic.

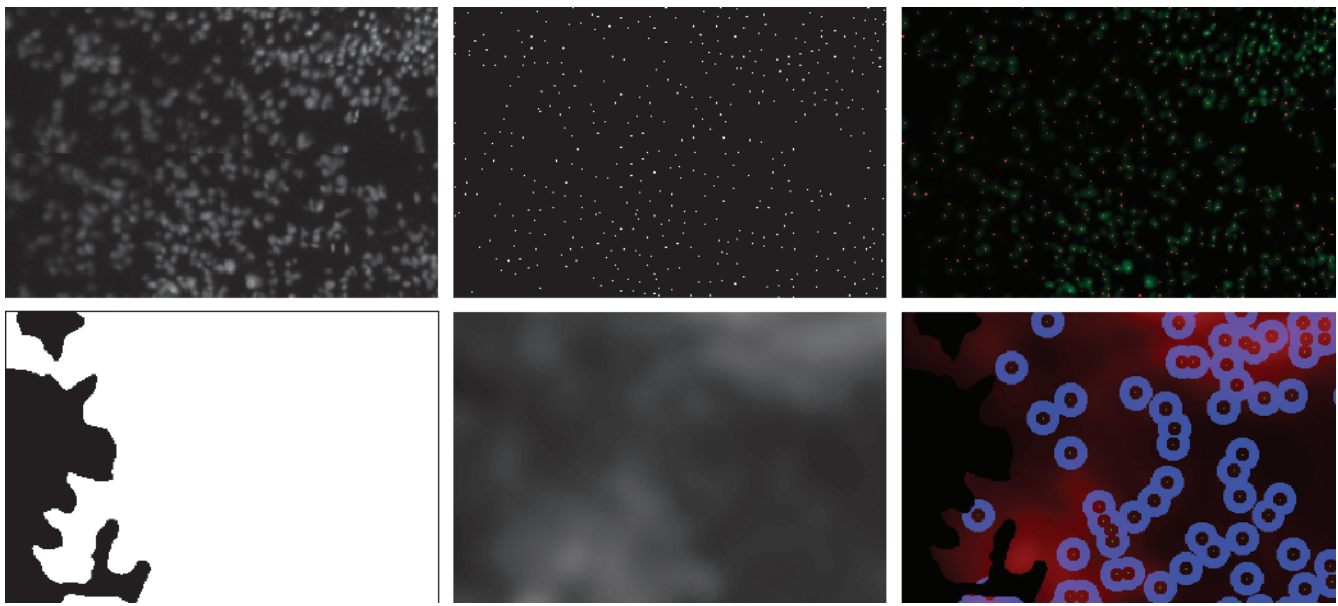


Figure 2. Analysis of EF5 value surrounding Ki-67+ cells: The upper left image depicts nuclei stained with Hoechst 33342 (the same process is done using Ki-67–stained cells, not shown). The upper central image is the point map that results from the counting algorithm described in text. A similar map is generated from the Ki-67 image (not shown). The upper right image shows the correlation between the counted points and the original Hoechst 33342 image. The mask shown in the lower left is generated from the upper left and middle images using the identified nuclei as reference points for cells and the base Hoechst image to threshold against. In combination, this yields an accurate map of viable tissue regions. The lower middle image shows the EF5 image after calibration and a Gaussian blur to eliminate hard edges and maintain the overall binding levels. The lower right image shows the combination of all images: the tissue mask has been applied to eliminate off tissue areas (black), calibrated EF5 binding levels are shown in varying intensities of red, green dots are Ki-67+ cells, and the blue rings are the 50- μ m regions around these cells in which the PO_2 levels are calculated.

21 mg/kg. Blood samples for drug levels were obtained before (control), 1 hour after drug administration, and at the time of surgery. Calculation of the drug concentration integrated with respect to time (area under the curve, AUC) was used to correct the absolute EF5 tissue binding level (IHC) for variations in drug dose and drug exposure time between patients [22].

Tissue Acquisition, Processing for EF5 Binding, and Analysis of EF5 Images

On the day after EF5 administration, tumors were surgically resected and placed in sterile, iced EXCELL 610 medium (JRH Biosciences, Lenexa, KS). In collaboration with the pathologist, tissue samples deemed unnecessary for clinical diagnosis were taken to the laboratory for processing and analysis.

IHC staining methods and quantitative fluorescence microscopy of EF5 in *in situ* tumor sections (Figure 1) and EF3 in tissue cubes for cube reference binding (CRB) were performed as reported previously [23]. CRB determination is an *in vitro* technique where millimeter-sized tissue cubes taken from an individual patient's tumors were incubated at 600 μ M/h in EF3, a sister drug of EF5, under controlled hypoxic conditions. The goal of this procedure was to determine the maximum level of EF3 binding possible for each patient's tumor. This technique allowed normalization of the *in situ* EF5 binding to each tumor's maximum binding value after correction for the AUC [22,23]. In addition to staining for EF5 alone, adjacent tissue sections were 1) costained for EF5 and Ki-67 (called EF5/Ki-67), as previously reported [24] (Figure 1), and 2) stained with "Competed Stain" (antibody mixed with 0.5 mM authentic EF5) to account for fluorescence

due to nonspecific staining (data not shown). The latter value was subtracted from the calculated value of *in situ* EF5 binding.

Images were analyzed using routines written in MatLab (The MathWorks, Inc, Natick, MA), whereby EF5-dependent fluorescence intensity values were sampled within an image (or part thereof) based on intact (viable) nuclei identified by a Hoechst 33342 mask [19] (Figure 2). Hoechst 33342 was applied to the slide immediately preceding imaging to stain the nuclei. The final EF5 intensity values were corrected for lamp intensity, individual patient AUC, and the competed stain value. The result of these corrections provided an EF5 binding value for each pixel, expressed as a percent of CRB (%CRB) [8,23]. We have converted %CRB into tissue PO_2 ranges using extensive data from *in vitro* studies [9,13,23,25].

To further characterize the image, cumulative frequency histograms of the %CRB of all the pixels in the image were calculated. Using this terminology, the median binding would be CF_{50} . To emphasize the most hypoxic cells, we used the CF_{95} value, wherein 95% of the cells have lower values and 5% have higher values. Thus, $CF_{95} = 20\%$ would mean that 95% of the EF5 values in the image were at or below 20% of maximum EF5 binding.

Proliferation Analysis

All images were loaded, preprocessed, and analyzed based on Hoechst 33342 and EF5/Ki-67 images for each tissue section (Figure 2). To correct for small misalignments due to wavelength shifts, the EF5/Ki-67 images were each aligned to the Hoechst 33342 image.

The Hoechst 33342 image was masked to reduce background noise using the Imtophat method (MatLab; The MathWorks, Inc). A threshold was applied to eliminate all pixels with an intensity value

below 0.005, yielding a black-and-white image mask. The resulting image was repeatedly (up to 1000 times) morphed with a majority transformation that turns any black pixel surrounded by five or more white pixels to white. This step filled in small areas that may have been missed by the previous threshold. The masks were reviewed individually at the end of the process to ascertain that the process was successful in capturing the features of the Hoechst 33342 image (Figure 2).

A counting algorithm was then applied to the EF5/Ki-67 and Hoechst 33342 images to identify each cell and to determine accurate counts of the number of total cells and of proliferating cells. To eliminate background values, the Imtophat filter was applied to both images. Each cell was identified in an iterative process. Each iteration included identification, centralization, and hole-punching steps (Figure 2). Identification was achieved by applying a threshold to the image that was at first highly discriminating and was gradually reduced in a quadratic fashion to a preset minimum value determined through repeated experimentation. Each of the identified objects was then “shrunk” to a point using a centralization process resulting in the replacement of the cell with a single pixel located at its centroid (center of mass). The hole punch completed the iteration, whereby the original image had a cell-sized (15 μm) disk centered on each centralized identified point removed from future iterative steps. This process resulted in a highly accurate cell count, as determined by hand counting in small areas (data not shown). The procedure used 30 iterations, with an initial threshold value of 1.00 decreasing to 0.03 in a quadratic fashion. These steps resulted in two new images termed *point maps*, one for Hoechst 33342 and one for the Ki-67 aspect of the EF5/Ki-67 images (Figure 2).

After the Hoechst 33342 and Ki-67 point maps were created, the correspondence between each Ki-67+ object and exactly one Hoechst 33342-identified nucleus was checked, for example, to confirm that the Ki-67-labeled objects were a strict subset of Hoechst 33342-labeled objects. To do this, we relied on the fact that the two point maps were generated from aligned images of the same tissue piece. A final point map was generated from the Hoechst 33342 point map where, for each Ki-67 point, the nearest Hoechst 33342 point was tagged as Ki-67+ (Figure 2). If a Ki-67+ point was not within 15 μm (roughly the size of a cell), then it was assumed that the anti-Ki-67 antibody had caused an artifact, which was then eliminated. This was found to be less than 1% of the cells examined (data not shown). Using this point map, our goal was to obtain information about the tissue oxygen level in the immediate vicinity of each Ki-67+ object. However, signal from the anti-Ki-67 was often very strong, and despite using a different fluorescent color to quantify EF5 binding, there was some bleed through from the Ki-67 dye (Cy3 vs Cy5, respectively). This represented a substantial signal in regions of low EF5 binding because EF5 binding is quantified over an intensity range spanning several decades [25]. To eliminate the Ki-67 fluorescence from calculation of the EF5 fluorescence surrounding the Ki-67+ cells, the fluorescence in the central regions of the area surrounding these cells was removed from analysis. Specifically, EF5 binding was assessed in a donut-shaped region centered on each Ki-67+ nucleus, with the central hole 15 μm in diameter and the overall diameter as 50 μm , excluding any pixels eliminated by the overall tissue mask (Figure 2).

The average EF5 value for the entire image (minus the center of the “donuts”) was calculated based on the overall tissue mask. Cumulative frequency graphs of EF5 binding in the tissue section being

evaluated *versus* near Ki-67+ cells was determined based on the 95th percentile of EF5 binding (CF_{95}). Final analyses were based on the CF_{95} values for the brightest slide evaluated for each patient as in our previously published studies [15,26,27].

Pathological Examination

All tissue sections were reviewed by a neuropathologist to confirm that the tissue section contained tumor. Tissue sections that contained less than 20% viable tumor or more than 80% normal tissue or necrosis were eliminated from further analysis. A minimum of three tissue sections from each patient was examined. The histologic diagnosis of the tumor in the EF5-stained tissue sections was compared with the pathologic diagnosis based on paraffin-embedded tissue sections. None of the EF5-stained tissue sections received a diagnosis that differed from that rendered clinically. A minimum of three tumor sections stained for EF5 and EF5/Ki-67 was examined for each patient.

Tumor Staging and Patient Outcome

The World Health Organization grade was based on pathological examination of the surgical specimen. Recurrence was determined by the treating physician based on magnetic resonance imaging studies (usually a change over time) and/or the examination of a pathological specimen from surgical re-resection or biopsy.

Statistical Methods

Descriptive statistics (frequency, percentage, mean, and SD) were used to report distributions of patient and tumor variables. Time to recurrence was defined from the date of EF5 administration (1 day preceding surgery) to the date of a documented event (recurrence or death due to any cause) or censored at last patient contact. For patients in whom a gross total resection was not obtained, time to recurrence was defined as the point at which tumor progression (i.e., growth) was identified on imaging. In two patients (nos. 32 and 58), the recurrence date could not be confirmed, so for analysis the date of recurrence was taken as the date of death. Overall survival was defined from the date of EF5 administration (1 day preceding surgery) or censored at the last patient contact. Potential prognostic factors considered in this analysis were the RPA classification [20,28], proliferation index (PI), EF5 (CF_{95}) binding in the vicinity of Ki-67+ cells, EF5 binding in the brightest tissue section examined ($\text{CF}_{95 \text{ max}}$), and a ratio of the latter two values. Survival analysis of the ratio were based on two cutoff points: (a) the 50% EF5 value for the ratio of $[\text{EF5/Ki-67}_{\text{binding}}]/[\text{Tumor}_{\text{binding}}]$ ($\text{Ratio}_{\text{EF5 } 50\%}$) and (b) the $\text{Ratio}_{\text{patients median value}}$ (=75.6%; Table 1).

The distributions of time to event outcomes were estimated by the method of Kaplan and Meier [29] and compared among patient groups defined by a prognostic factor using log-rank tests [30]. The independent prognostic value of a factor was evaluated using a multivariate Cox proportional hazards model [31]. Statistical significance was defined as $P < .05$. Borderline significance was defined as less than 0.10.

Results

Between September 2000 and November 2005, 17 patients with previously untreated GB (World Health Organization grade 4 gliomas) were entered into this clinical trial of EF5. One patient deteriorated

Table 1. Ratio Value Definitions and Details.

	Ratio Value Based on EF5 Value (Ratio _{EF5 50%})*	Ratio Value Based on No. Patients per Group (Ratio _{patients median}) [‡]
Cutoff points	50%	75.6%
No. patients below and above cutoff point	4 and 12	8 and 8
Significant for recurrence (univariate)?	Yes, $P = .0074$. The unadjusted hazard ratio is 10.5 (95% CI, 1.3-84.2).	No, $P = .17$. The unadjusted hazard ratio is 2.2 (95% CI, 0.7-6.8).
Significant for overall survival (univariate)?	Yes, $P = .0196$. The unadjusted hazard ratio is 5.2 (95% CI, 1.1-24.3).	Yes, $P = .038$. The unadjusted hazard ratio is 3.4 (95% CI, 1.1-11.0).
Significant for overall survival among RPA = 3 and 4 patients (univariate)? [‡]	Yes, $P = .048$. The unadjusted hazard ratio is 4.4 (95% CI, 0.9-21.1).	Borderline, $P = .059$. The unadjusted hazard ratio is 3.4 (95% CI, 0.89-13.3).
Significant for overall survival in multivariate analysis with RPA?	Yes, $P = .038$	Borderline, $P = .09$

*Ratio_{EF5 50%} = see text; note, based on brightest tissue section for each patient.

[‡]Ratio_{patients median} = see text; note, based on brightest tissue section for each patient.

[‡] $n = 12$, owing to elimination of patients with RPA = 5 from the analysis.

rapidly postoperatively and died of non-brain tumor-related causes preceding the onset of radiation therapy; this patient was not included in the analysis. Of the 16 remaining patients, 15 had died and 1 patient (no. 115) remained alive and without recurrence at the time of analysis. The patients' demographics and the details of their tumors and treatments are summarized in Table 2. The patients' mean age was 56.9 years (range, 23-77 years), with 12 males and 4 females. Fifteen patients were white and one patient was African American. There were 3, 9, and 4 patients with RPA levels of 3, 4, and 5, respectively (Table 2). Survival analysis confirmed that RPA classification was predictive of patient survival in this group of patients (RPA 3 and 4 *vs* RPA 5, $P = .0026$). Despite the small number of patients included in this trial, this finding confirms that these 16 patients are generally representative of patients with *de novo* GBs reported in the literature [28]. All patients received surgery with the intent of gross total resection followed by external beam radiation therapy (Table 2). In three patients, the actual radiation prescription could not be determined, although notes from the outside hospitals confirmed that full-course radiation therapy had been administered. In four patients, additional radiation was given at the time of recurrence by iodine 125 (¹²⁵I) monoclonal antibody treatment ($n = 1$) or Gliasite balloon ($n = 3$; Table 2). Administration of adjuvant therapy (chemotherapy, hormonal, or molecular therapy) either during or after initial radiation therapy or at the time of recurrence could be confirmed in 13 of 16 pa-

tients. Two patients received no adjuvant therapy, and this information was not available in one patient. Temozolomide, either during and/or after radiation, was administered in 11 patients. There was no relationship between temozolomide administration and outcome in this small patient group ($P > .05$).

All 16 gliomas contained regions of hypoxia, although the level and extent of hypoxia varied considerably between patients. As shown in Table 3, the most hypoxic region, CF_{95 max} in the 16 GBs ranged from 3.2% (mild hypoxia, PO₂ \approx 2.5%) to 26.7% (moderate hypoxia, PO₂ \leq 0.5%). On the basis of these data, most of the tumor cells in any of these tumors were at intermediate or high O₂ levels, and all tumors contained many cells that were physiologically oxidic. When analysis of patient outcome was performed based on the CF_{95 max} of EF5-alone-stained sections, this value was not predictive for either tumor recurrence or patient survival ($P > .05$).

Tissue sections were also costained with EF5/Ki-67 and analyzed for both PI and the EF5 values surrounding Ki-67+ cells (Figure 1 and Table 3). The PIs in this group of GBs ranged from 1.3% to 15.5% (median, 5%). Results of the survival analysis based on the PI or the EF5 values surrounding Ki-67+ cells were not significant for either recurrence or survival ($P > .05$).

As described above, two cutoff points were tested for evaluating the predictive value of the [EF5/Ki-67_{binding}]/[Tumor_{binding}] ratio: (a) Ratio_{EF5 50%} (4 patients below CF₉₅ = 50% and 12 patients above

Table 2. Patient Demographics, Tumor Characteristics, and Treatment Modalities.

Patient ID	Age/Race/Sex	Tumor Location	RPA Classification	Total Resection	Radiation Dose (Gy)*	Adjuvantive Chemotherapy
50	48/W/M	R parietal	3	Y	6120, ¹²⁵ I MAB	T, CCNU, Gliadel
115	50/AA/F	Parietal	4	N	6000	Irinotecan, LdT
39	49/W/M	R temporal	4	Y	6000	TAM, T
38	48/W/M	R temporal	3	Y	6000, Gliasite [†]	Gliadel
33	73/W/M	R temporal	4	Y	6100	T
74	69/W/F	R parietal	5	N	6000	T, LdT
42	67/W/F	R frontal	4	N	5940	T, TAM
55	52/W/M	L parietal	4	Y	5940	T, LdT
127	52/W/M	L > R corpus callosum	5	N	RDNR	INA
57	23/W/M	L frontal	3	Y	6000, Gliasite [†]	T, LdT
101	70/W/M	R temporal-occipital	5	Y	RDNR	T, LdT
123	55/W/M	R temporal-parietal	4	Y	6000, Gliasite [†]	T, LdT, CPT11, Avastin
52	77/W/M	L temporal	4	Y	6000	None given
107	51/W/F	R temporal	4	N	6000	T, LdT, CPT11, BMS
32	55/W/M	L parietal	5	N	RDNR	TAM
58	71/W/M	Corpus callosum	4	N	5940	None given

BMS indicates BMS-247550 (ixabepilone); CCNU, lomustine; CPT11, irinotecan; Gliadel, wafers impregnated with bis-chloronitrosourea (Carmustine); INA, information not available; LdT, low-dose temodar; RDNR, radiation dose not recorded because patient was treated at an outside hospital (however, notes confirmed that a full course of treatment was completed); T, temodar; TAM, tamoxifen; W, white.

*External beam.

[†]Gliasite = 6000 cGy at 1 cm.

Table 3. Patient Survival and Recurrence End Point Analyses.

Patient ID	Days Surviving	Days to Recurrence	CF ₉₅ max of Tissue Sections Examined, %	EF5 Value Near Ki-67+ Cells* (CF ₉₅), %	Ratio, † %	PI, ‡ %
50	677	235	7.9	1.0	12.4	2.8
115 [§]	1106	1106	5.0	1.5	30.5	2.8
39	1054	938	26.1	10.5	40.5	3.1
38	691	488	6.9	3.2	46.6	15.5
33	227	126	14.0	8.6	61.2	5.3
74	241	137	5.7	3.7	64.1	6.2
42	641	121	19.6	13.3	67.7	6.8
55	831	187	15.1	11.4	75.3	6.0
127	371	100	7.8	5.9	75.9	6.0
57	470	182	17.5	14.1	80.4	2.5
101	190	112	4.2	3.4	81.8	1.3
123	528	117	3.2	2.6	82.3	4.6
52	489	322	26.7	22.7	85.2	4.9
107	700	262	19.3	17.2	89.5	5.1
32	130	130	21.6	19.9	91.9	11.8
58	124	124	5.5	5.3	96.6	2.0

†Ratio = EF5 value near Ki-67+ cells (CF₉₅) / overall EF5 value (CF₉₅ max).
 ‡PI = number of Ki-67+ nuclei/total number of nuclei stained with Hoechst 33342.
 §This patient is still alive without recurrence.

CF₉₅ = 50%) and (b) Ratio_{patients median} (75.6%; 8 patients above and below this value) (Tables 1 and 3). Using the variable Ratio_{EF5 50%}, patients had a better prognosis if the ratio was less than 50%. This discriminator was predictive of both time to recurrence (*P* = .0074; Figure 3 and Table 1) and overall survival (*P* = .0196) (Figure 4A and Table 1). When considered along with RPA classification for overall survival (recurrence was not tested because RPA is not predictive of recurrence), the Ratio_{EF5 50%} was found to be an independent prognostic factor (*P* = .038).

Using Ratio_{patients median} as a discriminator, there was no predictive value for time to recurrence (*P* = .17; Table 1), but it was predictive for overall survival (*P* = .038) (Figure 4 and Table 1). When considered along with RPA classification, the Ratio_{patients median} value was found to be only borderline in its association with overall survival (HR = 2.8, *P* = .09).

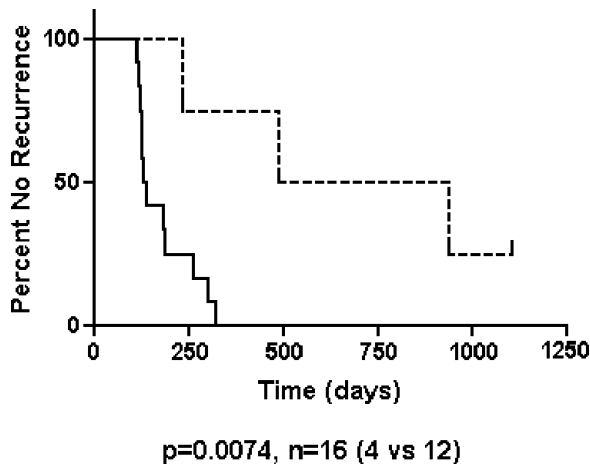


Figure 3. Analysis of time to tumor recurrence in 16 newly diagnosed GB patients based on their [EF5/Ki-67_{binding}]/[Tumor_{binding}] ratio. Patients with a Ratio_{EF5 50%} less than 50% (*n* = 4; dotted line) have a significantly longer time to recurrence than those with a Ratio_{EF5 50%} more than 50% (*n* = 12; solid line); *P* = .0074. Using the cutoff point of Ratio_{patients median}, this factor was not significant for recurrence (data not shown).

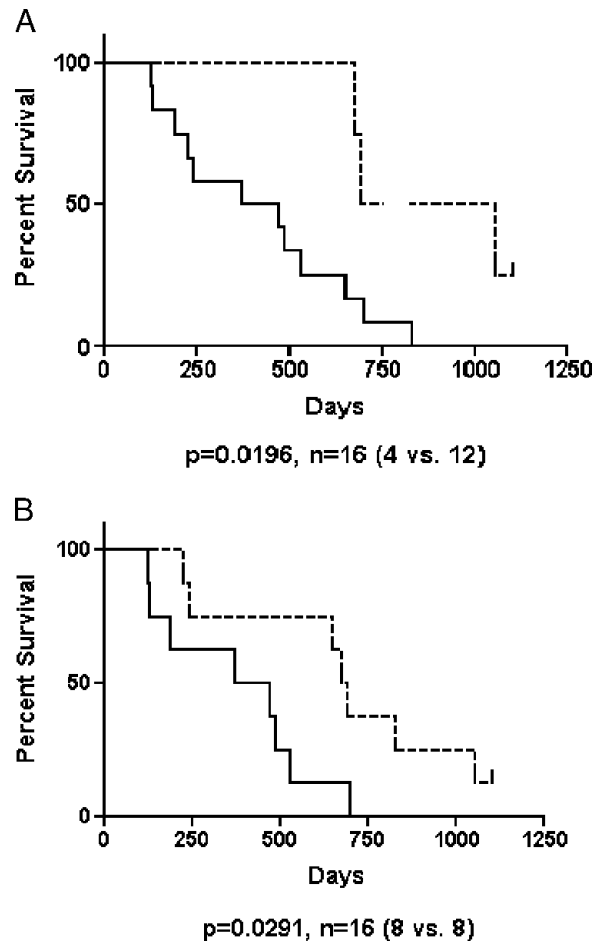


Figure 4. Analysis of time to patient survival in 16 newly diagnosed GB patients based on their [EF5/Ki-67_{binding}]/[Tumor_{binding}] ratio. (A) Patients with a Ratio_{EF5 50%} less than 50% (*n* = 4; dotted line) have a significantly longer time to recurrence than those with a Ratio_{EF5 50%} more than 50% (*n* = 12; solid line); *P* = .0196. (B) Comparing patients below and above of the Ratio_{patients median} value, patients had a significantly longer time to recurrence when this value was greater than the median (75.6%; *n* = 6); *P* = .0291 (dotted line).

In addition to performing a multivariate analysis, we performed a univariate analysis of $[EF5/Ki-67_{\text{binding}}]/[Tumor_{\text{binding}}]$ ratio values but only included the RPA class 3 or 4 ($n = 12$; Figure 5). Although this further reduces the sample size, the remaining patient subset was somewhat more homogeneous. This analysis will not answer the question of whether $[EF5/Ki-67_{\text{binding}}]/[Tumor_{\text{binding}}]$ ratio is an independent predictor of RPA but rather whether the predictive ability of this ratio will hold in patients with RPA = 3 or 4. Ratio_{EF5 50%} had a hazard ratio of 4.4 (95% confidence interval 0.90-21.1) and a significant log-rank test $P = .048$. Ratio_{patients median}, using cutoff point of 75.6%, had a hazard ratio of 3.4 (95% confidence interval [CI], 0.89-13.3) and a borderline significant log-rank test ($P = .059$; Table 1).

Discussion

In this pilot study, we have identified that GBs are characterized by varying degrees of hypoxia as assessed by EF5 binding and that most cells in GBs are either oxic or at intermediate levels of hypoxia. We have previously reported that EF5 binding generally increases with tumor grade when considering all types and grades of brain tumors [9,26], in keeping with our former studies in sarcomas [32]. This is in contrast to our studies in head and neck squamous cell carcinomas where tumor recurrence was associated with high EF5 binding irrespective of tumor grade [15]. Our results in brain tumors are distinct from previously published studies using Eppendorf needle electrodes [26,33,34]. We find that virtually all GBs contain some hypoxic regions, in comparison to grade 3 tumors that can contain rare regions of hypoxia and grade 2 tumors that are essentially oxic. Because our methods allow quantification of both the extent and degree of tissue hypoxia at a cellular resolution, our most general observation has been that all types of tumors contain physiologically oxic cells, with the main clinically relevant difference being the relative fraction of tissue existing under moderately or severely hypoxic conditions [15,26,32]. Thus, our central hypothesis has been that tumor aggressiveness is best characterized by the most hypoxic cells present,

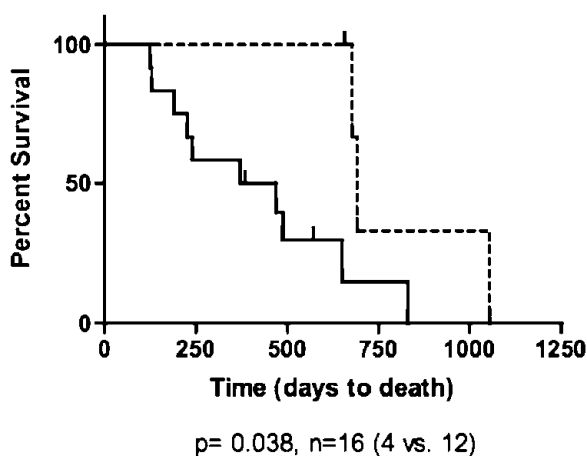


Figure 5. Multivariate analysis of 16 newly diagnosed GB patients based on their $[EF5/Ki-67_{\text{binding}}]/[Tumor_{\text{binding}}]$ ratio and their RPA classification. When considered along with RPA classification for overall survival, Ratio_{EF5 50%} was found to be an independent prognostic factor ($P = .038$). When considered along with RPA classification for overall survival, Ratio_{patients median} was found to be of borderline significance prognostic factor ($P = .09$). Dotted line = Ratio_{EF5 50%} > 50%, solid line = Ratio_{EF5 50%} < 50%.

and we have substantiated this in sarcomas, head and neck cancers, and high-grade glial brain tumors [15,26,32]. Our findings confirm studies in several other tumor types using other hypoxia measurement techniques [35–37]. However, this pilot study demonstrates that EF5 binding alone was not successful in predicting outcome for the small number of newly diagnosed GB patients studied herein.

We next considered PI as a means of predicting outcome in patients with GB. The PI contributes to prognosis for some tumor types (i.e., breast cancer [38] and squamous cell carcinomas of the oropharynx [39]) but has not consistently been associated with outcome in brain tumor patients [10–12]. This inconsistency should perhaps be expected. Non-cycling cells are known to be resistant to both chemotherapy and radiotherapy, and hypoxia can cause cells to exit the cell cycle [40,41]. However, rapid growth can contribute to a lack of tumor control, and it has been suggested that it is important to characterize a tumor's growth fraction before protracted treatments such as radiotherapy [42]. The balance between cell proliferation and death has been noted to be an important factor in determining overall tumor growth, and this consideration makes the understanding of the role of the PI, in the absence of quantification of the balancing factor cell death, complex [43].

Despite numerous investigations of hypoxia or proliferation individually, little is known about how these combined parameters (their quantitative and/or spatial relationships) contribute to outcome in human cancer. Several studies have combined analysis of endogenous markers of hypoxia in combination with proliferation markers in human cancers. One of the advantages of using endogenous hypoxia-associated markers (carbonic anhydrase 9, hypoxia-inducible factor 1, glucose transporter 1, and vascular endothelial growth factor) is that large retrospective studies using banked materials can be performed. However, all of these markers are known to measure factors in addition to tissue PO_2 [44]. Despite the expectation that proliferation would decrease with hypoxia, Saarnio et al. [45] showed expression of CA9 in areas of colorectal neoplasms with high proliferative capacity. Hoskin et al. [46] studied bladder cancer and found that proliferation was significantly higher in those tumors with the highest levels (>10%) of both GLUT1 ($P = .025$) and CA9 ($P = .029$) compared with those tumors that either were negative or had low levels of expression; colocalization studies were not performed because of the requirement to develop complex algorithms and methods. Neither the endogenous hypoxia markers nor PI (based on Ki-67) predicted for local control or metastases-free survival in this study. Hoogsteen et al. [47] studied CA9 and iododeoxyuridine (IdUrd) labeling in biopsies of head and neck squamous cell carcinomas, reporting that colocalization between IdUrd and CA9 ranged from 0% to 53%. The interpretation of the data in all of these studies is complicated by the absence of actual PO_2 values to correspond to the regions stained for endogenous markers. The study of Hoogsteen et al. used distance from blood vessels as a surrogate for tissue PO_2 ; the fraction of IdUrd-labeled cells positive for CA9 was highest at an intermediate distance from the blood vessels (100-150 μm). We have recently reported that in brain tumors, distance from blood vessels is not a good surrogate for oxygen partial pressure, as measured by EF5 binding [19]. Nonetheless, the fraction of IdUrd-labeled cells that were also positive for CA9 in the head and neck cancer study of Hoogsteen et al. correlated with the worst disease-free survival rates ($P = .04$). The latter observation parallels the findings reported herein.

Nordmark et al. [48] studied tumor oxygenation in human sarcomas using polarographic oxygen needle electrodes, proliferation,

and potential doubling time (T_{pot}) with iododeoxyuridine flow cytometry and IHC. There was a significant correlation between the median PO_2 and the tumor cell potential doubling time ($P = .041$). Interestingly, the fastest proliferating tumor cells were found in the poorest oxygenated soft tissue sarcomas.

Studies have been performed using pimonidazole as a hypoxia marker in human colorectal [18], head and neck [17], bladder [16,46], and cervical cancers [49,50]. In some studies, colocalization of pimonidazole and proliferation markers was found [17,18], and in others, there was an inverse relationship between these end points [50]. In bladder cancers [16], increased vessels in pimonidazole-positive areas and increased numbers of proliferating cells near these vessels were reported. The percentage of IdUrd-positive cells in pimonidazole-positive areas were not associated with survival in head and neck cancer [51].

The $Ratio_{EF5\ 50\%}$ was initially selected for analysis because there was a clear break in the data between patient 38 ($[EF5/Ki-67_{binding}]/[Tumor_{binding}]$ ratio = 46.6) and patient 33 (ratio value = 61.2; Table 3). The selection of a $Ratio_{EF5\ 50\%}$ between these values seemed appropriate in the absence of any comparative data analysis of this type in the literature. In addition, a cutoff point based on physiologic measurements seemed more meaningful than a statistical value of 50% of patients above or below a random ratio value ($Ratio_{patients\ median}$; Table 3). Considering a $Ratio_{patients\ median}$ of 75.6%, the values immediately above and below only differ by 0.3 (75.3% and 75.9%). These are very unlikely to be physiologically different because this difference is beyond the accuracy of the measurement techniques. Nonetheless, we present both data sets because the $Ratio_{patients\ median}$ is commonly used in the literature. The results of the analyses of both cut points are similar although not identical (Table 1).

We find that for the most aggressive tumors (12/16 patients; $EF5_{EF5\ 50\%} > 50\%$), irrespective of the Ki-67+ fraction and degree of hypoxia found, there was virtually no overall relationship between hypoxia and the presence of Ki-67+ cells. That is, the distribution of EF5 binding around Ki-67+ cells was not different from that of the rest of the tumor. In contrast, for the less aggressive tumors (4/16; $Ratio_{EF5\ 50\%} < 50\%$), Ki-67+ cells had a distribution of EF5 binding values that was lower (e.g., these cells were relatively oxic) compared with the tumor tissue as a whole. The findings were similar when the $Ratio_{patients\ median}$ was considered. The observation related to most aggressive *versus* less aggressive tumors represents a subtle difference, made possible only by the quantitative nature of EF5 binding calculations. The impact of this difference was significant, even using multiparametric analysis combined with RPA; $Ratio_{EF5\ 50\%}$ was a predictor for tumor recurrence and patient survival in the therapy-responsive patients. Because of this, we thought it important to bring these results forward despite the pilot nature of this study. In addition, the new image analysis methods described herein should be very useful in the evaluation of EF5-stained tissues or other marker binding. We propose that this result may help elucidate basic mechanisms of GB aggressiveness.

Because the methods described in this report are new, we do not know whether other tumor types will behave like GBs. Indeed, it is not certain what to expect because there are no previous studies where proliferation data have been colocalized with the actual PO_2 of Ki-67+ cells.

A characteristic feature of GBs is the presence of infarcted vessels leading to the phenomenon of pseudopalisading necrosis [52]. If much of the hypoxia found in GBs were related to these (presumably) irreversible blockages of blood flow, then perhaps the PO_2 of

dividing cells reflects the physiological consequences of the pseudopalisade formation (i.e., trapping of the cells) rather than a specific effect on cell cycling. If this were true, then the aggressiveness of the tumor might relate to the frequency and extent of vessel infarction leading to a higher probability of trapping cycling cells in these volumes; this may lead to the impression that the PO_2 around these cells was similar to that of the tumor as a whole. Tumor vessel infarction has been commonly described in GB [52], and abnormalities of the clotting cascade are not uncommon in patients with any malignant tumor type, especially in patients with GB. There is an interesting discussion in the literature arising from the observation of Brat and van Meier about whether cells actively invade toward or away from these infarcts. Our observations are more in keeping with the latter.

Currently, an understanding of the factors that cause cells in tumors to exist in a cycling *versus* noncycling state (proliferative “P” *vs* quiescent “Q” [53]) is incomplete. “Q” cells were originally thought to arise from insufficient supply of cytokines or nutrients, including oxygen. Data from *in vitro* studies are not very informative because cell growth is virtually unaffected by oxygen tensions of 0.2% or even less (considered as “severe” hypoxia) [40,41,54]. Current thinking about the cycling status of individual tumor cells would undoubtedly invoke a multitude of molecular signaling mechanisms affecting many physiologies in the tumor, as well as that of supporting tissue cells and tumor stem cells. However, studies of oxygen dependence of such phenomena under carefully controlled and monitored conditions have not been performed. The data presented in this report emphasize the importance of detailed evaluations on PO_2 both *in vitro* and *in vivo*. An important clinical ramification of our results is that there may not be a consistent or general relationship between absolute PO_2 and inhibition of cell cycling, suggesting that tumor aggressiveness is modulated by the PO_2 dependence of cell cycling in individual tumors. Our observations and hypotheses are undergoing further testing and study.

In summary, the understanding of why GBs are treatment-resistant remains poor despite decades of research. The predictive factors currently in use rely on various clinical and pathological factors determined in a detailed statistical analysis, for example, RPA [18]. In many cancers, hypoxia and/or proliferation are documented prognostic factors but not in GBs. This pilot study identifies a unique interaction between these factors and seems to show prognostic importance for recurrence and survival, independent of RPA status. Three translationally relevant insights are provided in this article:

- 1) Hypoxia is always found in GBs, and therefore, its measurement, treatment targeting, and modification are likely to have important roles in patient's evaluation and therapy.
- 2) Future studies are necessary to identify the mechanisms of the findings herein, particularly whether they are the result of molecular modifications of tumor metabolism or a temporal vascular phenomenon. On the basis of these results, specific therapies might be developed.
- 3) Future prognostic studies must evaluate the biology (including molecular) and physiology of individual tumors rather than emphasize differences between patient groups.

Acknowledgments

The authors thank Deborah Smith and Susan Prendergast, Associate Directors of Clinical Research, for their help in patient care and Deirdre P. Magarelli for her initial studies related to this project.

References

- [1] Stupp R, Dietrich PY, Ostermann Kraljevic S, Pica A, Maillard I, Maeder P, Meuli R, Janzer R, Pizzolato G, Miralbell R, et al. (2002). Promising survival for patients with newly diagnosed glioblastoma multiforme treated with concomitant radiation plus temozolomide followed by adjuvant temozolomide. *J Clin Oncol* **20**, 1375–1382.
- [2] Wen PY and Kesari S (2008). Malignant gliomas in adults. *N Engl J Med* **359**, 492–507.
- [3] Brahimi-Horn MC, Chiche J, and Pouyssegur J (2007). Hypoxia and cancer. *J Mol Med* **85**, 1301–1307.
- [4] Evans SM and Koch CJ (2003). Prognostic significance of tumor oxygenation in humans. *Cancer Lett* **195**, 1–16.
- [5] Shannon AM, Bouchier-Hayes DJ, Condrum CM, and Toomey D (2003). Tumour hypoxia, chemotherapeutic resistance and hypoxia-related therapies. *Cancer Treat Rev* **29**, 297–307.
- [6] Loges S, Mazzone M, Hohensinner P, and Carmeliet P (2009). Silencing or fueling metastasis with VEGF inhibitors: angiogenesis revisited. *Cancer Cell* **15**, 167–170.
- [7] Fernandez Y, Espana L, Manas S, Fabra A, and Sierra A (2000). Bcl-xL promotes metastasis of breast cancer cells by induction of cytokines resistance. *Cell Death Differ* **7**, 350–359.
- [8] Deryugina E and Quigley J (2006). Matrix metalloproteinases and tumor metastasis. *Cancer Metastasis Rev* **25**, 9–34.
- [9] Evans S, Judy K, Dunphy I, Jenkins W, Nelson P, Collins R, Wiley E, Jenkins K, Hahn S, Stevens C, et al. (2004). Comparative measurements of hypoxia in human brain tumors using needle electrodes and EF5 binding. *Cancer Res* **64**, 1886–1892.
- [10] Brown DC and Gatter KC (2002). Ki67 protein: the immaculate deception? *Histopathology* **40**, 2–11.
- [11] Torp SH (2002). Diagnostic and prognostic role of Ki67 immunostaining in human astrocytomas using four different antibodies. *Clin Neuropathol* **21**, 252–257.
- [12] Bouvier-Labit C, Chinot O, Ochi C, Gambarelli D, Dufour H, and Figarella-Branger D (1998). Prognostic significance of Ki67, p53 and epidermal growth factor receptor immunostaining in human glioblastomas. *Neuropathol Appl Neurobiol* **24**, 381–388.
- [13] Koch CJ (2002). Measurement of absolute oxygen levels in cells and tissues using oxygen sensors and 2-nitroimidazole EF5. *Methods Enzymol* **352**, 3–31.
- [14] Koch CJ, Evans SM, and Lord EM (1995). Oxygen dependence of cellular uptake of EF5 [2-(2-nitro-1H-imidazol-1-yl)-N-(2,2,3,3,3-pentafluoropropyl)acetamide]: analysis of drug adducts by fluorescent antibodies vs bound radioactivity. *Br J Cancer* **72**, 869–874.
- [15] Evans SM, Du KL, Chalian AA, Mick R, Zhang PJ, Hahn SM, Quon H, Lustig R, Weinstein GS, and Koch CJ (2007). Patterns and levels of hypoxia in head and neck squamous cell carcinomas and their relationship to patient outcome. *Int J Radiat Oncol Biol Phys* **69**, 1024–1031.
- [16] Hoskin PJ, Sibtain A, Daley FM, Saunders MI, and Wilson GD (2004). The immunohistochemical assessment of hypoxia, vascularity and proliferation in bladder carcinoma. *Radiother Oncol* **72**, 159–168.
- [17] Wijffels KI, Marres HA, Peters JR, Rijken PF, van der Kogel AJ, and Kaanders JH (2008). Tumour cell proliferation under hypoxic conditions in human head and neck squamous cell carcinomas. *Oral Oncol* **44**, 335–344.
- [18] van Laarhoven HW, Kaanders JH, Lok J, Peeters WJ, Rijken PF, Wiering B, Ruers TJ, Punt CJ, Heerschap A, and van der Kogel AJ (2006). Hypoxia in relation to vascularity and proliferation in liver metastases in patients with colorectal cancer. *Int J Radiat Oncol Biol Phys* **64**, 473–482.
- [19] Ranelli N, Evans SM, and Judy KD (2009). Role of hypoxia in human brain tumors. *Neurosurg Q* **19**(1), 1–12.
- [20] Curran WJ Jr, Scott CB, Horton J, Nelson JS, Weinstein AS, Fischbach AJ, Chang CH, Rotman M, Asbell SO, and Krisch RE (1993). Recursive partitioning analysis of prognostic factors in three Radiation Therapy Oncology Group malignant glioma trials [see comments]. *J Natl Cancer Inst* **85**, 704–710.
- [21] Urtasun RC, Chapman JD, Feldstein ML, Band RP, Rabin HR, Wilson AF, Marynowski B, Starreveld E, and Shnitka T (1978). Peripheral neuropathy related to misonidazole: incidence and pathology. *Br J Cancer Suppl* **3**, 271–275.
- [22] Koch CJ, Hahn SM, Rockwell K Jr, Covey JM, McKenna WG, and Evans SM (2001). Pharmacokinetics of EF5 [2-(2-nitro-1H-imidazol-1-yl)-N-(2,2,3,3,3-pentafluoropropyl)acetamide] in human patients: implications for hypoxia measurements *in vivo* by 2-nitroimidazoles. *Cancer Chemother Pharmacol* **48**, 177–187.
- [23] Evans SM, Hahn S, Pook DR, Jenkins WT, Chalian AA, Zhang P, Stevens C, Weber R, Weinstein G, Benjamin I, et al. (2000). Detection of hypoxia in human squamous cell carcinoma by EF5 binding. *Cancer Res* **60**, 2018–2024.
- [24] Evans S, Hahn S, Magarelli D, and Koch C (2001). Hypoxic heterogeneity in human tumors: EF5 binding, vasculature, necrosis and proliferation. *Am J Clin Oncol* **24**, 467–472.
- [25] Koch CJ (2008). Importance of antibody concentration in the assessment of cellular hypoxia by flow cytometry: EF5 and pimonidazole. *Radiat Res* **169**(6), 677–688.
- [26] Evans S, Judy K, Dunphy I, Jenkins W, Nelson P, Collins R, Wiley E, Jenkins K, Hahn S, Stevens CW, et al. (2004). Comparative measurements of hypoxia in human brain tumors using needle electrodes and EF5 binding. *Cancer Res* **64**, 1886–1892.
- [27] Evans SM (2006). Oxygen levels in normal and previously irradiated human skin as assessed by EF5 binding. *J Invest Dermatol* **126**, 2596–2606.
- [28] Scott CB, Scarantino C, Urtasun R, Movsas B, Jones CU, Simpson JR, Fischbach AJ, and Curran WJ Jr (1998). Validation and predictive power of Radiation Therapy Oncology Group (RTOG) recursive partitioning analysis classes for malignant glioma patients: a report using RTOG 90-06. *Int J Radiat Oncol Biol Phys* **40**, 51–55.
- [29] Kaplan E and Meier P (1958). Nonparametric estimation from incomplete observations. *J Am Stat Assoc* **4**, 57–81.
- [30] Mantel N (1966). Evaluation of survival data and two new rank order statistics arising in its consideration. *Cancer Chemother Rep* **50**, 163–170.
- [31] Cox D (1972). Regression models and life tables. *J R Stat Soc Series B Stat Methodol* **34**, 187–220.
- [32] Evans SM, Fraker DL, Hahn SM, Gleason K, Jenkins WT, Jenkins K, Hwang W-T, Zhang P, and Koch CJ (2006). EF5 binding and clinical outcome in human soft tissue sarcomas. *Int J Radiat Oncol Biol Phys* **64**(3), 922–927.
- [33] Lally BE, Rockwell S, Fischer DB, Collingridge DR, Piepmeier JM, and Knisely JP (2006). The interactions of polarographic measurements of oxygen tension and histological grade in human glioma [see comment]. *Cancer J* **12**, 461–466.
- [34] Rampling R, Cruickshank G, Lewis AD, Fitzsimmons SA, and Workman P (1994). Direct measurement of PO₂ distribution and bioenergetic enzymes in human malignant brain tumors. *Int J Radiat Oncol Biol Phys* **29**, 427–431.
- [35] Brizel DM, Sibley GS, Prosnitz LR, Scher RL, and Dewhurst MW (1997). Tumor hypoxia adversely affects the prognosis of carcinoma of the head and neck. *Int J Radiat Oncol Biol Phys* **38**, 285–289.
- [36] Gatenby RA, Kessler HB, Rosenblum JS, Coia LR, Moldofsky PJ, Hartz WH, and Broder GJ (1988). Oxygen distribution in squamous cell carcinoma metastases and its relationship to outcome of radiation therapy. *Int J Radiat Oncol Biol Phys* **14**, 831–838.
- [37] Vanselow B, Eble MJ, Rudat V, Wollensack P, Conradt C, and Dietz A (2000). Oxygenation of advanced head and neck cancer: prognostic marker for the response to primary radiochemotherapy. *Otolaryngol Head Neck Surg* **122**, 856–862.
- [38] Railo M, Nordling S, von Boguslawsky K, Leivonen M, Kyllonen L, and von Smitten K (1993). Prognostic value of Ki-67 immunolabelling in primary operable breast cancer. *Br J Cancer* **68**, 579–583.
- [39] Grabenbauer GG, Muhlfriedel C, Rodel F, Niedobitek G, Hornung J, Rodel C, Martus P, Iro H, Kirchner T, Steininger H, et al. (2000). Squamous cell carcinoma of the oropharynx: Ki-67 and p53 can identify patients at high risk for local recurrence after surgery and postoperative radiotherapy. *Int J Radiat Oncol Biol Phys* **48**, 1041–1050.
- [40] Papandreou I, Powell A, Lim AL, and Denko N (2005). Cellular reaction to hypoxia: sensing and responding to an adverse environment. *Mutat Res* **569**, 87–100.
- [41] Koch CJ, Kruuv J, and Frey HE (1973). The effect of hypoxia on the generation time of mammalian cells. *Radiat Res* **53**, 43–52.
- [42] Thomlinson RH (1982). Measurement and management of carcinoma of the breast. *Clin Radiol* **33**, 481–493.
- [43] Evan GI and Vousden KH (2001). Proliferation, cell cycle and apoptosis in cancer. *Nature* **411**, 342–348.
- [44] Moon EJ, Brizel DM, Chi JT, and Dewhurst MW (2007). The potential role of intrinsic hypoxia markers as prognostic variables in cancer. *Antioxid Redox Signal* **9**, 1237–1294.
- [45] Saarnio J, Parkkila S, Parkkila AK, Haukipuro K, Pastorekova S, Pastorek J, Kairaluoma MI, and Karttunen TJ (1998). Immunohistochemical study of colorectal tumors for expression of a novel transmembrane carbonic anhydrase, MN/CA IX, with potential value as a marker of cell proliferation. *Am J Pathol* **153**, 279–285.
- [46] Hoskin PJ, Sibtain A, Daley FM, and Wilson GD (2003). GLUT1 and CAIX as intrinsic markers of hypoxia in bladder cancer: relationship with vascularity and proliferation as predictors of outcome of ARCON. *Br J Cancer* **89**, 1290–1297.
- [47] Hoogsteen IJ, Marres HA, Wijffels KI, Rijken PF, Peters JR, van den Hoogen FJ, Oosterwijk E, van der Kogel AJ, and Kaanders JH (2005). Colocalization of

- carbonic anhydrase 9 expression and cell proliferation in human head and neck squamous cell carcinoma. *Clin Cancer Res* **11**, 97–106.
- [48] Nordsmark M, Hoyer M, Keller J, Nielsen OS, Jensen OM, and Overgaard J (1996). The relationship between tumor oxygenation and cell proliferation in human soft tissue sarcomas. *Int J Radiat Oncol Biol Phys* **35**, 701–708.
- [49] Varia MA, Calkins-Adams DP, Rinker LH, Kennedy AS, Novotny DB, Fowler WC Jr, and Raleigh JA (1998). Pimonidazole: a novel hypoxia marker for complementary study of tumor hypoxia and cell proliferation in cervical carcinoma. *Gynecol Oncol* **71**, 270–277.
- [50] Kennedy AS, Raleigh JA, Perez GM, Calkins DP, Thrall DE, Novotny DB, and Varia MA (1997). Proliferation and hypoxia in human squamous cell carcinoma of the cervix: first report of combined immunohistochemical assays. *Int J Radiat Oncol Biol Phys* **37**, 897–905.
- [51] Wijffels KI, Kaanders JH, Rijken PF, Bussink J, van den Hoogen FJ, Marres HA, de Wilde PC, Raleigh JA, and van der Kogel AJ (2000). Vascular architecture and hypoxic profiles in human head and neck squamous cell carcinomas. *Br J Cancer* **83**, 674–683.
- [52] Brat DJ, Castellano-Sanchez AA, Hunter SB, Pecot M, Cohen C, Hammond EH, Devi SN, Kaur B, and Van Meir EG (2004). Pseudopalisades in glioblastoma are hypoxic, express extracellular matrix proteases, and are formed by an actively migrating cell population. *Cancer Res* **64**, 920–927.
- [53] Kal HB (1973). Proliferation behaviour of P and Q cells in a rat rhabdomyosarcoma after irradiation as determined by DNA measurements. *Eur J Cancer* **9**, 753–756.
- [54] Koch CJ, Kruuv J, Frey HE, and Snyder RA (1973). Plateau phase in growth induced by extreme hypoxia. *Int J Radiat Biol* **23**, 67–74.